

Cell Reports Methods, Volume 3

Supplemental information

**Single-cell sequencing of individual
retinal organoids reveals
determinants of cell-fate heterogeneity**

Amy Tresenrider, Akshayalakshmi Sridhar, Kiara C. Eldred, Sophia Cuschieri, Dawn Hoffer, Cole Trapnell, and Thomas A. Reh

Supplemental Information

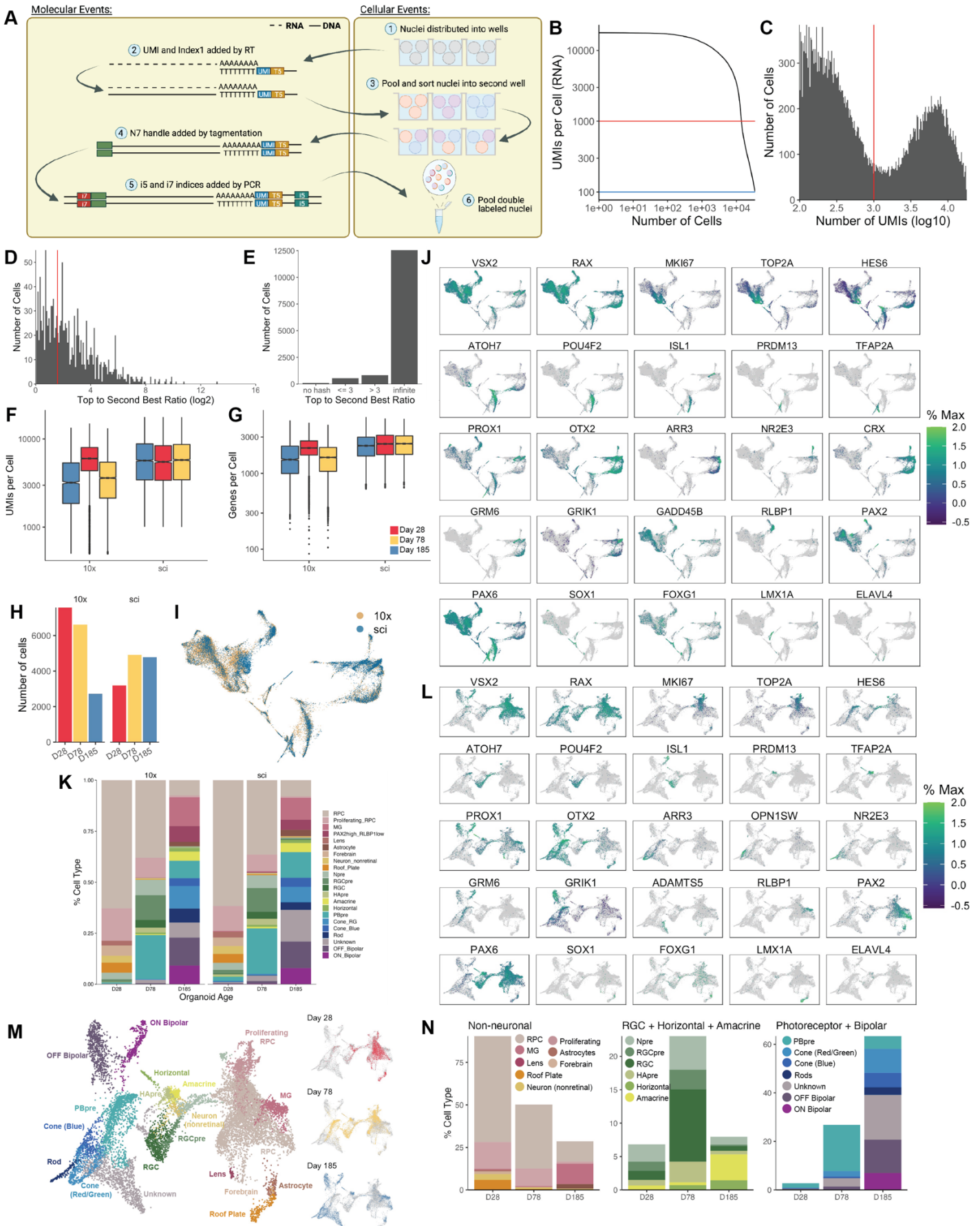
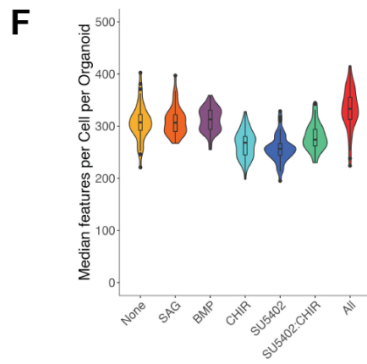
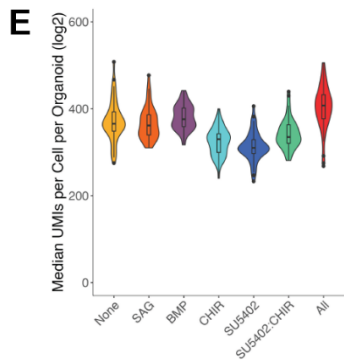
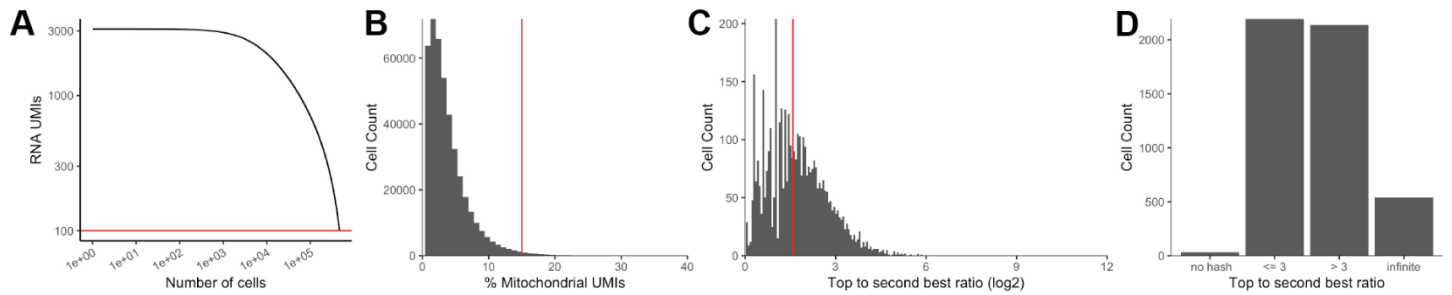


Figure S1. Quality control of sci-Plex and 10x comparison datasets, related to Figure 1. **A)** sci-RNA-seq relies on successive split-pool barcoding of RNA: permeabilized nuclei are distributed into wells of a 96-well plate. Reverse transcription is performed using a polyD-T oligo that contains both a UMI and barcode (T5). Each well is provided a unique oligo such that all cDNA molecules produced in a well will have the same barcode. Cells are then pooled and redistributed into a second set of 96-well plates. The cDNA is converted to dsDNA and subjected to tagmentation which adds a uniform sequence to the end of the cDNA molecules. This sequence and the sequence at the end of the RT oligos can be used to amplify the library by PCR. The PCR primers each contain barcode sequences (i7, i5) and the wells all receive a unique combination of PCR oligos. Experiments can be designed such that the vast majority of cells travel through a unique set of wells. Thus, RNAs that share the same barcode combination are assumed to have come from the same cell. **B)** A knee plot of the number of UMIs per cell compared to the number of cells recovered. The red line (1000UMIs) indicates the value denoting whether a barcode combination should be considered a cell. **C)** A histogram of the number of cells per UMI count. UMI counts left of the red line (1000 UMIs) are removed from the analysis. **D)** Hashes were sequenced and assigned to cells. A Top to Second Best Ratio was then calculated by dividing the UMI count of the most common hash barcode by the UMI count of the second most common hash barcode detected for an individual cell. A histogram of the number of cells recovered at each Top to Second Best Ratio was then generated. The red line (3) denotes the Top to Second Best Ratio required for a cell to be assigned a confident hash call. **E)** A bar plot of the number of cells with Top to Second Best Ratios matching given criteria. In the event only a single hash barcode is detected, the ratio is infinite. **F)** Bar plots of the number of cells recovered for each sample. **G)** Box plots of the number of UMIs recovered from each cell for each sample. **H)** Box plots of the number of genes recovered from each cell for each sample. **I)** Integration of 10x and sci data by Seurat's MNN-CCA methodology. The cells are colored by the technology with which they were prepared for sequencing. **J)** Feature plots of the genes used to define cell types from the integrated sci-Plex and 10x UMAP. **K)** Stacked bar plots demonstrating the cell type compositions of organoids from D28, D78, and D185 organoids as prepared for sequencing by 10x and sci-Plex. RPC: retinal progenitor cell, MG: Müller glia, Npre: retinal neuronal precursor, RGC: retinal ganglion cell, RGCpre: RGC precursor, HApri: horizontal/amacrine precursor, PBpre: photoreceptor/bipolar precursor, Cone_RG: red/green cone. **L)** A UMAP was generated by Monocle3 using only the cells recovered by sci-Plex. Cells are colored by expression of the indicated gene. The displayed genes were used when defining cell types. **M)** The UMAP from L). Left: Cells are colored by cell type, Right: Cells are faceted and colored by organoid age. **N)** Using the cell type assignments from M, cell types were split into Brain/Non-neuronal (Non-neuronal), RGC+Horizontal+Amacrine (RGC+H+A), and Photoreceptor+Bipolar (PR+BP) categories. Cells were counted and the % Cell Type was determined for each organoid age.



G

sci-Plex oligo plate	Condition 1	Condition 2
1	None	SAG
2	SU5402	CHIR
3	SU5402:CHIR	BMP
4	All	

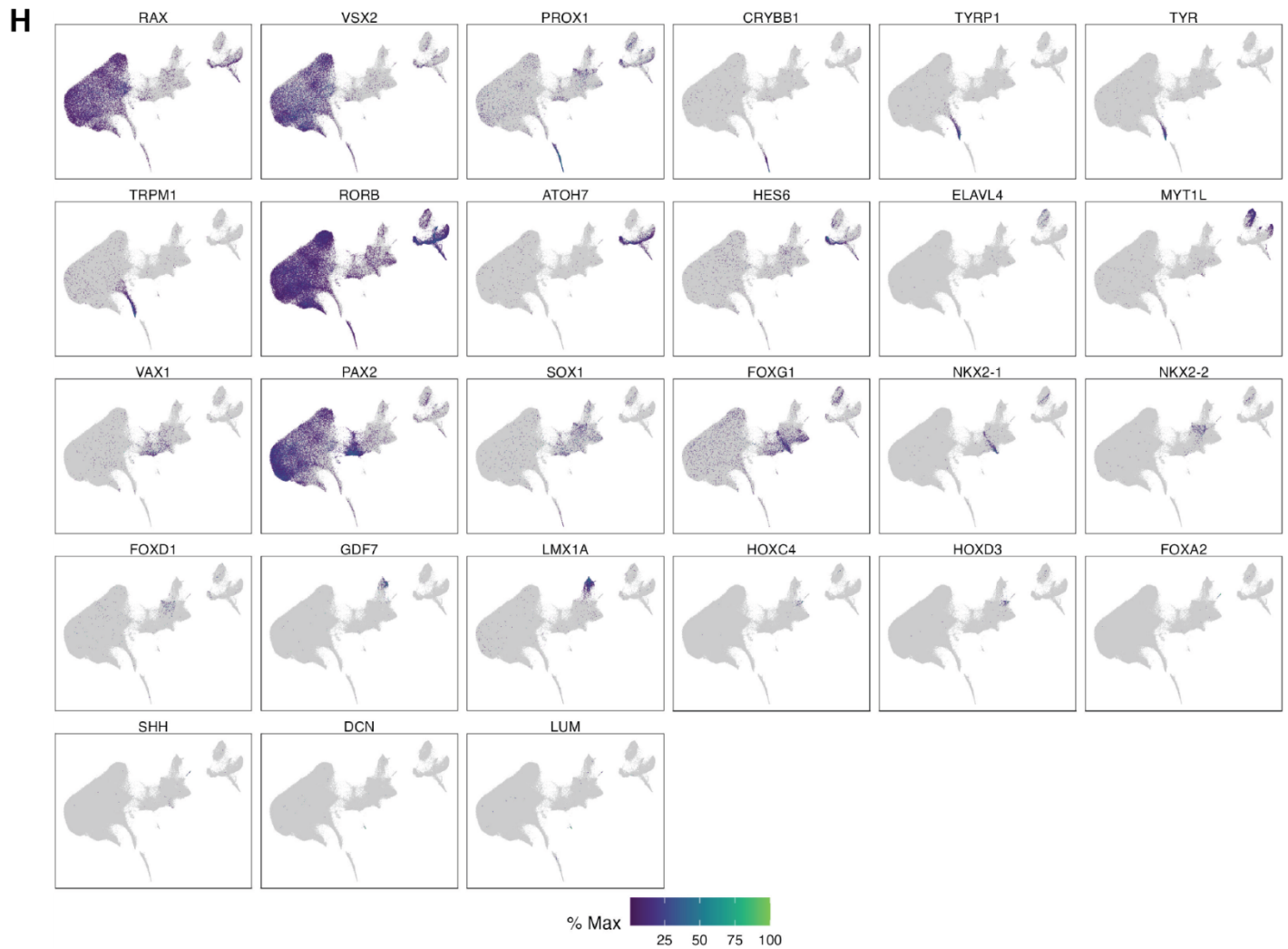


Figure S2. Quality control of sci-Plex performed on individual D28 organoids, related to Figure 2. **A)** A knee plot of the number of UMIs per cell compared to the number of cells recovered from D28 organoids. The red line (100 UMIs) indicates the value denoting whether a barcode combination should be considered a cell. **B)** A histogram of the % mitochondrial UMIs. Cells with percentages right of the red line (15%) are removed from the analysis. **C)** A histogram of the number of cells recovered at each Top to Second Best Ratio was then generated. The red line (2.5) denotes the Top to Second Best Ratio required for a cell to be assigned a confident hash call. In the event only a single hash barcode is detected, the ratio is infinite. **D)** A bar plot of the number of cells with Top to Second Best Ratios matching given criteria. **E)** Violin plots of the number of UMIs recovered from each cell for each D28 organoid per treatment. **F)** Violin plots of the number of features recovered from each cell for each D28 organoid per treatment. **G)** Table indicating which sci-Plex oligo plate was used to hash each of the treatment conditions. **H)** Expression plots of the genes used to define the cell types in Figure 2E.

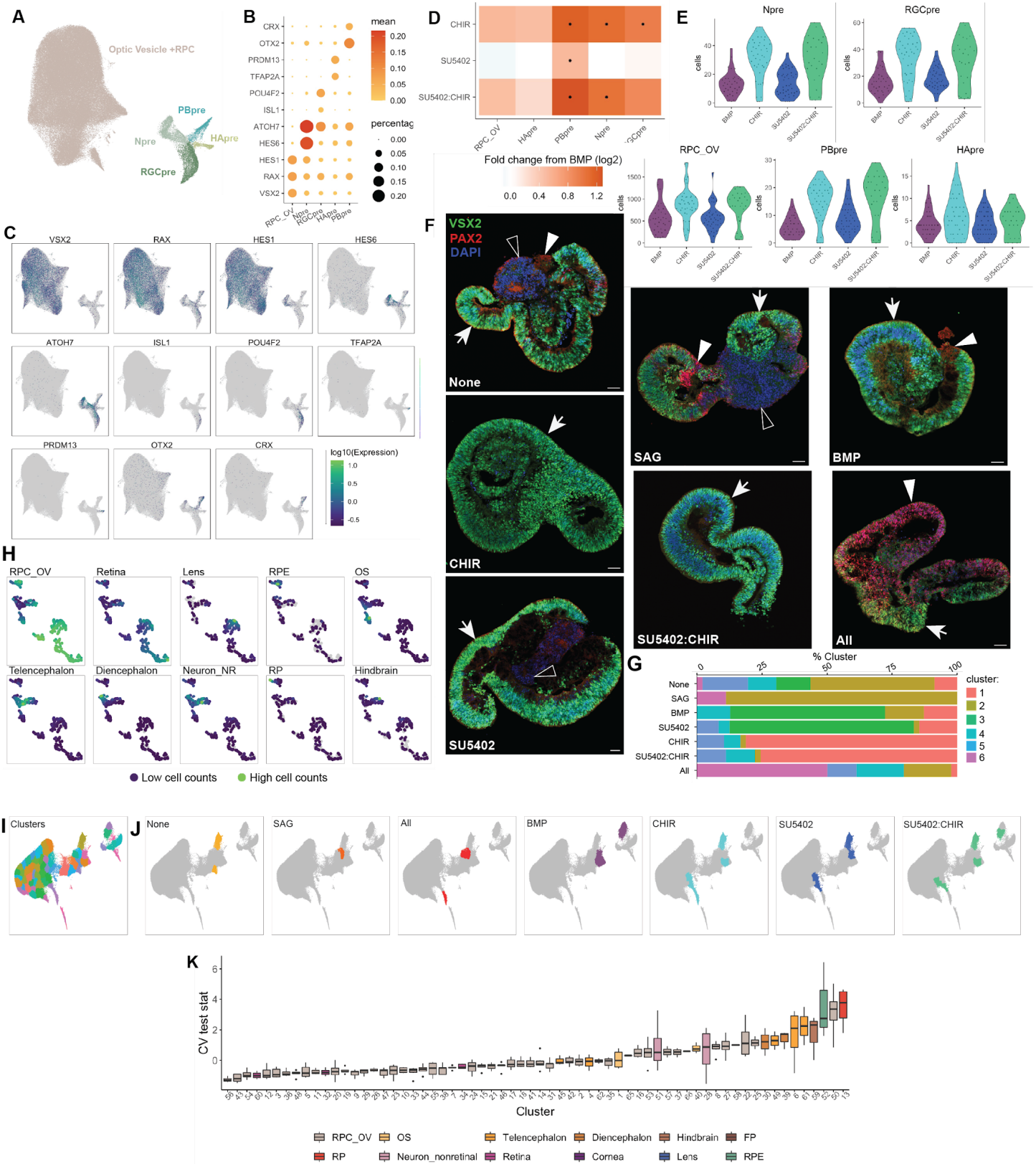


Figure S3. Investigation of abundance changes in specific retinal cell types and cell types with high variability, related to Figure 3. A) A UMAP of the Retina and RPC_OV subset of cells from D28 organoids was derived by Monocle3. Cells are colored by retinal cell type. RPC_OV: retinal progenitor cell/optic vesicle,

Npre: retinal neuronal precursor, RGCpre: retinal ganglion cell precursor, HApr: horizontal/amacrine precursor, PBpre: photoreceptor/bipolar precursor. **B)** A dot plot of the genes used to identify the retinal cell types in A. **C)** Expression plots of the genes used to define the cell types in Figure S4A. **D)** Heatmap of fold change in cell type abundance compared to “BMP” for D28 organoids. A beta-binomial model was fit to the data and used to determine whether there were significant changes in cell type abundances. A * in the center of the box indicates a q-value of less than 0.05 after Benjamini Hochberg correction. Note that while only the retinal cell types are displayed, the test was performed on size-factor normalized cell counts of all cell types in the organoid. **E)** Violin plots of size-factor normalized cell counts for the retinal cell types. Plots are colored by treatment. **F)** Immunostaining of D28 organoids with VSX2 (RPCs/Npre, green), PAX2 (OS, red), and DAPI (blue). Scale bar represents 50 μm . Arrow = RPCs/Npre, empty arrow head = non-optic-stalk (OS), filled arrow head = OS. **G)** Stacked bar plot demonstrating the distribution of organoids across archetypes. **H)** UMAP from 3M in which color indicates the abundance of each cell type. Each dot represents an individual organoid. Blue indicates few cells of that type are found in that organoid and green indicates high counts for that cell type. RPC_OV: retinal progenitor cell/optic vesicle, RPE: retinal pigmented epithelium, OS: optic stalk, Neuron_NR: non-retinal neuron, RP: roof plate. **I)** UMAP from 2C of the individual clusters used for analyses modeling the variance across treatments and clusters. **J)** UMAP highlighting the clusters with significantly higher variance than expected in None, SAG, All, BMP, CHIR, SU5402, and SU5402:CHIR. **K)** Box plots with clusters ordered according to increasing CV test stat. A single CV test stat is calculated for each treatment, and the boxplots summarize the CV test stat values across treatments for each cluster. Box plots are colored by the cell type assignment as in Figure 2E. RPC_OV: retinal progenitor cell/optic vesicle, RPE: retinal pigmented epithelium, OS: optic stalk, RP: roof plate, FP: floor plate.

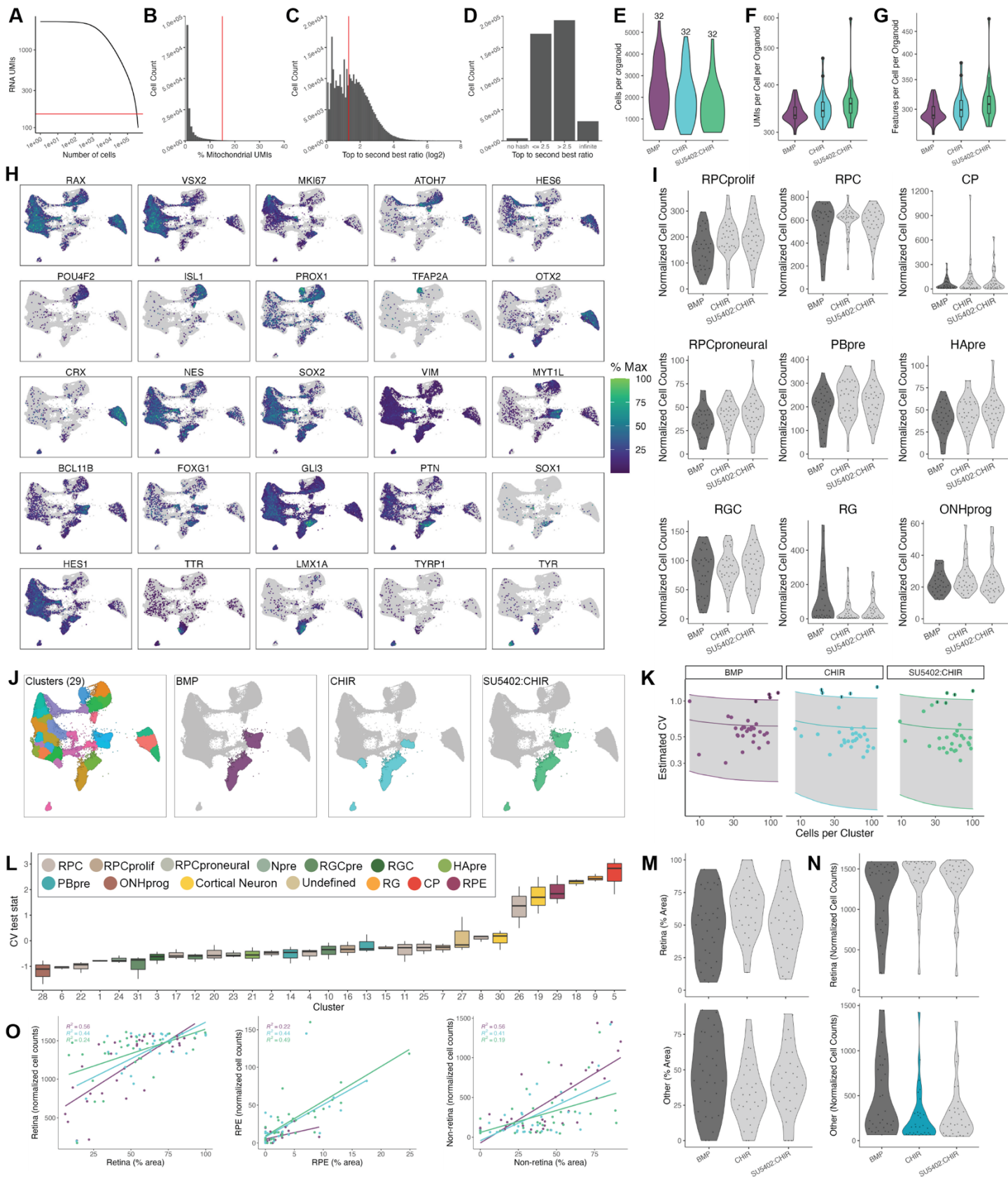


Figure S4. Quality control of the D63 organoid datasets, related to Figure 4. **A)** A knee plot of the number of UMIs per cell compared to the number of cells recovered. The red line (150 UMIs) indicates the value denoting whether a barcode combination should be considered a cell. **B)** A histogram of the number of cells per % mitochondrial UMIs. All cells with > 15% were discarded. **C)** A histogram of the number of cells recovered at each Top to Second Best Ratio was then generated. The red line (2.5) denotes the Top to Second Best Ratio required for a cell to be assigned a confident hash call. **D)** A bar plot of the number of cells with Top to Second Best Ratios matching given criteria. In the event only a single hash barcode is detected, the ratio is infinite. **E)** Violin plot of the number of cells recovered for each organoid across treatments. **F)** Violin plot of the number of UMIs recovered from each cell per D63 organoid per treatment. **G)** Violin plot of the number of features recovered from each cell per D63 organoid per treatment. **H)** Expression plots of the genes used to define cell types in Figure 5A. **I)** Violin plots of size-factor normalized cell counts for D63 organoids. The dark gray indicates the treatment that was used for fold-change calculations in 5B, and light gray indicates no significant change in cell type abundance. **J)** A beta-binomial distribution was used to determine the dispersions across treatments for each of the 29 clusters used to define cell types. The mean and CV calculated from the beta-binomial distribution, were then used to model the relationship between the number of cells per cluster and the CV using a gamma distribution. Left: UMAP with the cells colored by the 29 clusters used to define cell types. Right: UMAPs in which the clusters highlighted are more variable across treatments than expected by chance. Cells are colored by treatment. **K)** Displayed are the modeled relationships between mean cell count and CV per cluster colored by treatment. **L)** Boxplots with clusters ordered according to increasing CV test stat. A single CV test stat is calculated for each treatment, and the boxplots summarize the CV test stat values across treatments. RPC: retinal progenitor cell, RPCprolif: proliferating RPC, RPCproneural: proneural RPC, Npre: retinal neural precursor, RGC: retinal ganglion cell, RGCpre: RGC precursor, HApr: horizontal/amacrine precursor, PBpre: photoreceptor/bipolar precursor, ONHprog: optic nerve head progenitor, RG: radial glia, CP: choroid plexus, RPE: retinal pigmented epithelium. **M)** Violin plots of % Area measurements for Retina and Non-retinal (Other) cell types as calculated from bright phase microscopy images of D62 organoids. Plots are colored as in S6H. **N)** Violin plots of size-factor normalized Retina and Non-retinal (Other) cell counts for D63 organoids using broad cell types. Plots are colored as in S6H with teal indicating a significantly decreased cell type abundance. **O)** Scatter plots showing the correlation between the sci-Plex cell counts and % Area for each individual D63 organoid across treatments. R^2 values are in the top right corner colored by treatment.

Table S1. Cost benefit analysis between sci-Plex and 10x*, related to Figure 1.

Experiment	Total cells	sci-Plex cost per cell	10x cost per cell	sci-Plex cost per sample prep	10x cost per sample prep
10x match	16,914 (10x) 12,867 (sci)	\$0.14	\$0.35**	\$608	\$2000*
D28	203,511	\$0.04	\$0.30***	\$23	\$196***
D63	194,335	\$0.11	\$0.0625***	\$76	\$232***

* This analysis does not take into account the sequencing cost. However, sci usually results in fewer UMIs which can make it difficult for some gene expression analyses, but it does make it easier to sequence for a lower cost.

**This was the actual cost for the experiment as performed. Each age was loaded onto its own lane with a desired recovery of 7000 cells per well.

***This estimate assumes multiplexing of 16 samples per lane using the CellPlex kit. A desired recovery of 500 cells per sample (8000 cells per lane) was assumed for the D28 experiment and 2000 cells per sample for the D63 experiment (32,000 cells per lane). These values are based off of the median number of cells recovered per organoid from the sci-Plex experiments.

Table S2. Cell type marker genes, related to Figures 1-4.

A list of the genes used to assign cell types for all sci-Plex experiments

Cell Type	Expt	Enriched Markers								
RPC	10x_sci comp	VSX2	RAX							
Proliferating RPC	10x_sci comp	VSX2	RAX	MKI67	TOP2A					
MG	10x_sci comp	RLBP1								
PAX2high RLBP1low	10x_sci comp	PAX2	RLBP1							
Lens	10x_sci comp	PROX1	CRYBB1							
Astrocyte	10x_sci comp	PAX2	GFAP							
Forebrain	10x_sci comp	SOX1	FOXP1							
Neuron nonretinal	10x_sci comp	ELAVL4	DLX6	MYT1L						
Roof plate	10x_sci comp	GDF7	LMX1A							
Npre	10x_sci comp	HES6	ATOH7							
RGCpre	10x_sci	ATOH7	POU4F2							

	comp								
RGC	10x_sci comp	POU4F2	ISL1						
HApré	10x_sci comp	PRDM13	TFAP2A						
Amacrine	10x_sci comp	TFAP2A							
Horizontal	10x_sci comp	PROX1	TFAP2A	ONECUT1					
PBpre	10x_sci comp	HES6	OTX2	CRX					
Cone RG	10x_sci comp	ARR3	CRX	OTX2					
Cone Blue	10x_sci comp	OPN1SW	CRX	OTX2					
Rod	10x_sci comp	NRL	CRX	OTX2					
Unknown	10x_sci comp	PIK3CG	PP1R27	GDF15	KBTBD12	INPP5D	OTX2		
OFF Bipolar	10x_sci comp	VSX1	GRIK1	OTX2					
ON Bipolar	10x_sci comp	VSX2	ISL1	PROX1	GRM6	OTX2			
RPC/OV	D28 All cells	RAX	VSX2	HES1					
OS	D28 All cells	VAX1	PAX2	SOX1					
Telencephalon	D28 All cells	SOX1	FOXG1	NKX2-1					
Diencephalon	D28 All cells	SOX1	FOXD1	NKX2-2					
Hindbrain	D28 All cells	HOXC4	HOXD3	HOXB6					
FP	D28 All cells	FOXA2	SHH						
RP	D28 All cells	GDF7	TTR	LMX1A					
Neuron nonretinal	D28 All cells	ELAVL4	MYT1L	EOMES	FOXG1				
Retina	D28 All cells	RORB	ATOH7	ONECUT2	HES6	RAX			
Cornea	D28 All cells	DCN	LUM						
Lens	D28 All cells	PROX1	CRYBB1						
RPE	D28 All cells	TYRP1	TYR	TRPM1	OTX2				
RPC/OV	D28 Retina	RAX	VSX2	HES1					
Npre	D28 Retina	HES6	ATOH7						
RGCpre	D28 Retina	ATOH7	POU4F2	ISL1					
HApré	D28 Retina	TFAP2A	PRDM13						
PBpre	D28 Retina	OTX2	CRX						

RPC	D63	RAX	VSX2	RORB						
RPCprolif	D63	RAX	VSX2	MKI67	TOP2A	RORB				
RPCproneural	D63	MKI67	TOP2A	ATHO7	HES6	RORB	ONECUT1			
Npre	D63	ATHO7	HES6	RORB	ONECUT1					
RGCpre	D63	ATHO7	POU4F2	RORB	ONECUT1					
RGC	D63	POU4F2	ISL1	RORB	ONECUT1					
HApr	D63	PROX1	TFAP2A	PRDM13	RORB	ONECUT1				
PBpre	D63	OTX2	CRX	ONECUT1	RORB					
ONHprog	D63	NES	SOX2	VIM	SOX1	RAX	VSX2	MKI67	TOP2A	RORB
Transition	D63	N/A								
Cortical Neuron	D63	MYT1L	BCL11B							
Radial Glia	D63	GLI3	FOXP1	SOX1	PTN	SOX2	HES1	PPRX1	OTX1	
Choroid Plexus	D63	TTR	LMX1A	WNT2B	WNT3A	OTX2				
RPE	D63	TYRP1	TYR	OTX2	MITF					